Proceedings of the PHOTON-2017 Conference, Geneva, Switzerland, 22 – 26 May 2017, edited by David d'Enterria, Albert de Roeck and Michelangelo Mangano, CERN Proceedings, Vol. 1/2018, CERN-Proceedings-2018-001 (CERN, Geneva, 2018)

Photon+V measurements in ATLAS

D.V. Krasnopevtsev on behalf of ATLAS collaboration
National Research Nuclear University MEPhI, Moscow, Russia

Abstract
ATLAS measurements of multi-boson production processes involving isolated photons in proton–proton collisions at 8 TeV are summarized. Standard Model cross sections are measured with high precision and are compared to theoretical predictions. No deviations from Standard Model predictions are observed and limits are placed on parameters used to describe anomalous triple and quartic gauge boson couplings.

Keywords
Standard Model; photons; weak gauge bosons; ATLAS; aTGC; aQGC; VBS.

1 Introduction

Photon+V ($V = W, Z$) studies are used to test the electroweak sector of the Standard Model (SM) with high accuracy using multi-boson production cross sections. These measurements allow to probe the $SU(2)_L \times U(1)_Y$ gauge symmetry of the electroweak theory that determines the structure and self-couplings of the vector bosons and to search for signs of new physics using anomalous triple and quartic gauge-boson coupling (aTGC and aQGC) studies. Moreover precision photon+V measurements affect tuning of Monte-Carlo (MC), which describes some backgrounds in SM and beyond the SM studies.

The ATLAS detector [1] uses electromagnetic calorimeter (EM) and inner detector (ID) tracking system to reconstruct photons with high efficiencies. Both photons that do or do not convert to electron-positron pairs are reconstructed in ATLAS. The EM calorimeter is composed of three sampling layers longitudinal in shower depth. The fine η granularity of the strips in the first layer is sufficient to provide discrimination between single photon showers and two overlapping showers coming from the decays of neutral hadrons in jets. The jet suppression is about 10^4 during the first operation period of Large Hadron Collider (LHC) [2].

The measurements in this paper use 20.3 fb^{-1} of proton–proton collisions collected with the ATLAS detector during LHC operation at a center-of-mass energy of 8 TeV. Standard Model cross sections for $V\gamma$ production in ATLAS were measured with high accuracy already with 7 TeV data. Proton-proton collisions at 8 TeV allowed to improve these measurements and provided an opportunity to study rare processes of $Z\gamma$ scattering and triboson productions.

2 Standard Model Photon+V measurements

2.1 $Z\gamma(\gamma)$ production

$Z\gamma(\gamma)$ production includes electroweak (EWK) and quantum chromodynamics (QCD) components. QCD component is studied using charged and neutral Z decays with initial and final state radiation photons: $Z/\gamma^* \to \ell^+\ell^-\gamma(\gamma)$ (where ℓ = e or μ) and $Z \to \nu\bar{\nu}\gamma(\gamma)$. The measurements are compared to SM predictions obtained with a parton-shower MC simulation and with two higher-order perturbative parton-level calculations at next-to-leading order (NLO) [3] and next-to-next-to-leading order (NNLO) [4].

The Z/γ^* decays to charged leptons are selected using high transverse momentum (p_{T}) electrons or muons triggers and photons with transverse energy $E_{\mathrm{T}} > 15$ GeV. Events with Z boson decays to neutrinos are selected using high E_{T} photon triggers: $E_{\mathrm{T}} > 130$ GeV for the single photon channel and $E_{\mathrm{T}} > 22$ GeV for the di-photon channel. In this analysis events with any number of jets are considered (inclusive case) as well as events with veto on jets with $p_{\mathrm{T}} > 30$ GeV (exclusive case). Selected

https://doi.org/10.23727/CERN-Proceedings-2018-001.229

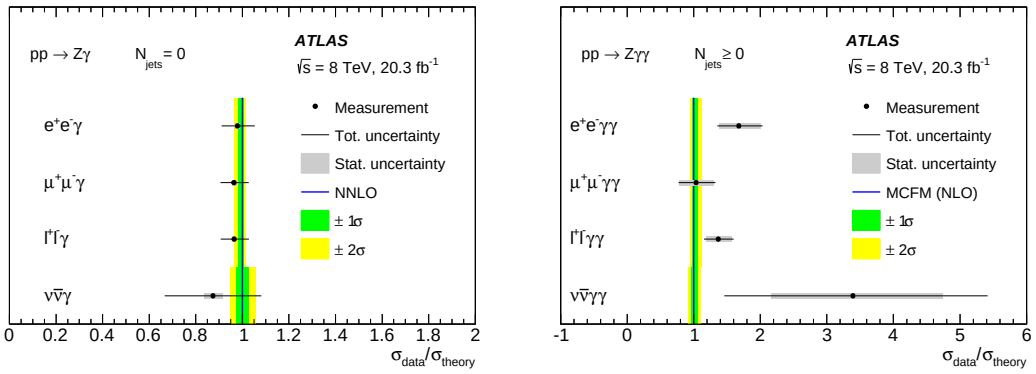

(a) (b)

Fig. 1: Comparison between the measured cross sections and the NNLO theory predictions in the exclusive region for the $pp \to Z\gamma$ (left) and NLO theory predictions in the inclusive region for the $pp \to Z\gamma\gamma$ (right) [5].

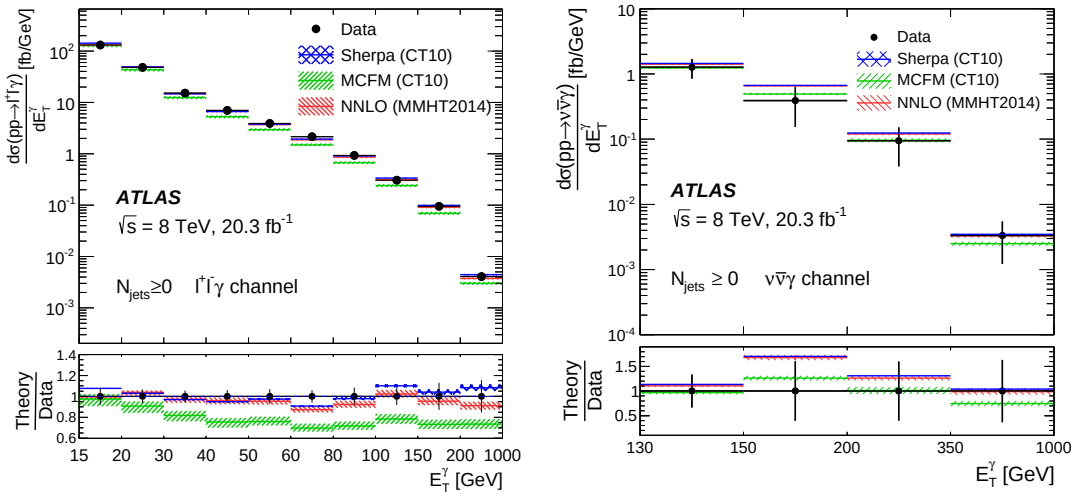

(a) (b)

Fig. 2: The measured (points with error bars) and expected differential cross sections as a function of E_{T}^{γ} for the pp$\to \ell^+\ell^-\gamma$ process (left) and the pp$\to \nu\bar{\nu}\gamma$ process (right) in the inclusive fiducial regions. The lower plots show the ratios of various theory predictions to data (shaded bands) [5].

$\ell^+\ell^-\gamma(\gamma)$ event candidates must contain exactly one pair of same-flavor, opposite-charge isolated leptons (electrons or muons) with invariant di-lepton mass ($m_{\ell^+\ell^-}$) greater than 40 GeV and at least one or two isolated photons. $Z\gamma(\gamma)$ events with neutrino Z decay are selected by considering events with $E_{\mathrm{T}}^{\mathrm{miss}} > 100$ GeV (110 GeV for the di-photon channel) and at least one or two isolated photons. $E_{\mathrm{T}}^{\mathrm{miss}}$ is the absolute value of the vector of momentum imbalance in the transverse plane and is used to identify neutrinos in this study. The separation between the reconstructed photon (di-photon system) direction and missing energy vector in the transverse plane is required since in signal events the Z boson should recoil against the photon(s). To suppress $W(\gamma)$+jets and $W\gamma(\gamma)$ backgrounds, events containing a muon or an electron are rejected.

The backgrounds in $Z\gamma(\gamma)$ signal regions are dominated by events in which jets and electrons are misidentified as photons. In neutrino channels additionally there is contribution from events where jet energy is not totally measured causing deviations in missing energy value. The largest background contributions are determined using data-driven techniques, smaller are obtained with a MC simulation.

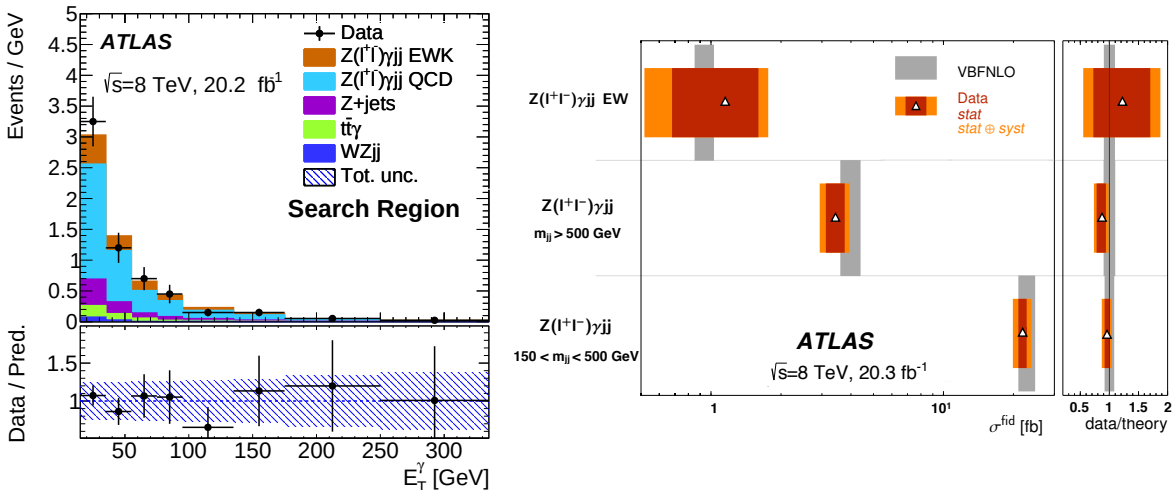

(a) (b)

Fig. 3: $Z\gamma$ centrality - (a) and comparison between the measured cross sections and NLO theory predictions for different control regions - (b) for $Z(\ell\ell)\gamma$ channel in $Z\gamma$ VBS analysis [6].

The measured cross sections are compared to the SM predictions. There is generally a good agreement between the measured cross sections in the $Z\gamma$ channels and those predicted by the SM. NNLO calculation of the inclusive cross section for the $Z(\ell^+\ell^-)\gamma$ channel is in a better agreement with the measurement than the NLO calculation. The results for both charged and neutrino $Z\gamma\gamma$ channels are compared to the NLO MCFM predictions. Although the observed number of events is not large, the combined $\ell^+\ell^-\gamma\gamma$ results show 5 standard deviations over non-signal hypothesis. Figure 1 shows the level of agreement between the experimental results and the theory for all channels.

Differential cross sections measurements are performed in $Z\gamma$ channels to remove measurement inefficiencies and resolution effects from the observed distributions. Figure 2 shows the measured and the predicted by the SM E_{T}^{γ} distributions for $pp \to \ell^+\ell^-\gamma$ and $pp \to \nu\bar{\nu}\gamma$ events with the inclusive selection. Better agreement is found with NNLO predictions.

2.2 $Z\gamma$ scattering

EWK processes in $Z\gamma$ production are characterized by jets with wide rapidity separation, large di-jet invariant mass and production with high centrality. Vector boson scattering (VBS) belongs to EWK component and can be selected by presence of two high energetic jets in addition to bosons. Therefore only events with more than 1 jet are considered in this analysis. Jets are considered if they have $p_{\mathrm{T}} > 30$ GeV and $|\eta| < 4.5$. Jet candidates are rejected if they are not well separated from the previously selected leptons and photons. Both charged and neutral decays of Z are studied. $Z(\ell\ell)\gamma$ channel is used for cross section measurements and search for aQGCs, while $Z(\nu\nu)\gamma$ is used only in the search for aQGC. Figure 3(a) shows the distribution of centrality for observed $Z\gamma$ events in the search region for charged channel. Data (full dots) demonstrates reasonable agreement with background and signal predictions.

Signal events in charged channel should contain two same flavour and opposite sign leptons with $p_{\mathrm{T}}^{e,\mu} > 25$ GeV, isolated photon with $E_{\mathrm{T}}^{\gamma} > 15$, $m_{\ell\ell} > 40$ GeV and $m_{\ell\ell\gamma} + m_{\ell\ell\gamma} > 182$ GeV. Two regions are studied in the analysis. The search region with maximum VBS contribution and invariant di-jet mass (m_{jj}) greater than 500 GeV is aimed to measure EWK and EWK+QCD cross sections. The control region with maximum QCD contribution and $150 < m_{jj} < 500$ GeV is used to normalize QCD contribution in the search region and to perform EWK+QCD cross sections measurements. Figure

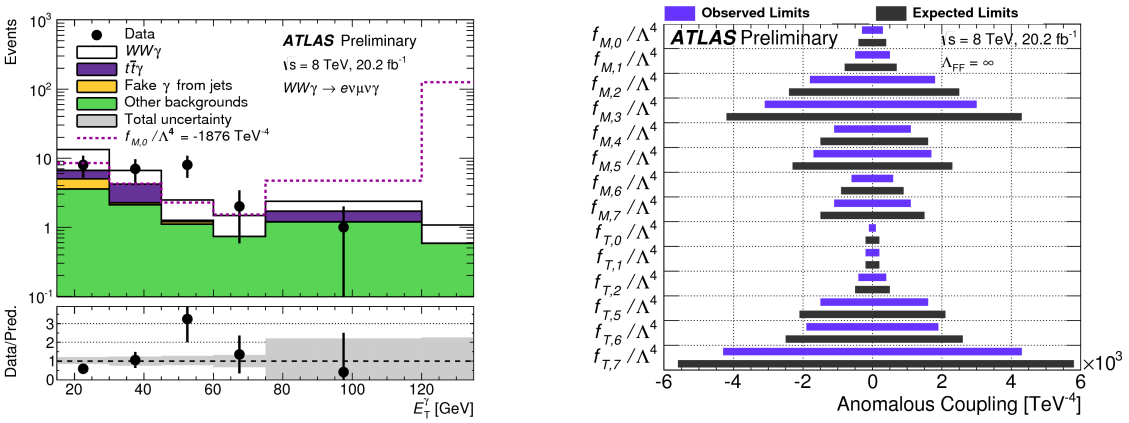

(a) (b)

Fig. 4: Transverse energy distributions for photons in $e\nu\mu\nu\gamma$ channel (left) and the observed from $WV\gamma$ analysis ununitarized limits for the studied aQGC parameters (right) [7]. The dashed purple line on left plot shows contribution from aQGC in case f_{M0}/Λ^4 parameter is set to be -1876 TeV^{-4}.

		Observed limit [fb]	Expected limit [fb]	σ_{theo} [fb]
Fully leptonic	$e\nu\mu\nu\gamma$	3.7	$2.1^{+0.9}_{-0.6}$	2.0
Semileptonic	$e\nu jj\gamma$	10	16^{+6}_{-4}	2.4
	$\mu\nu jj\gamma$	8	10^{+4}_{-3}	2.2
	$\ell\nu jj\gamma$	6	$8.4^{+3.4}_{-2.4}$	2.3

Fig. 5: Observed and expected cross-section upper limits at 95% CL for the different $WV\gamma$ final states. The expected cross-section limits are computed assuming no signal is present. The last column shows the theory prediction computed with the VBFNLO [7].

3(b) summarizes all cross section measurements made in this analysis. The left part of the plot shows exact values, while the right side illustrates data to theory ratio. The significance of the observed EWK production signal is 2σ.

2.3 $WV\gamma$ production

$WV\gamma$ production is studied using fully leptonic $WW\gamma$ and and semi-leptonic $WV\gamma$ channels. Bosons in these channels originate from quartic or triple (with initial radiation photon) vertices or come from radiative processes.

$WW\gamma$ events are studied solely in the $e\nu\mu\nu\gamma$ final state since others fully-leptonic channels have low sensitivity because of large $Z\gamma$ backgrounds. The $e\nu\mu\nu\gamma$ event candidates are selected by considering events with $E_{\text{T}}^{\text{miss}} > 15$ GeV, one isolated photon with $E_{\text{T}}^{\gamma} > 15$ GeV, one electron and one muon with $p_{\text{T}} > 20$ GeV and $m_{\ell\ell} > 50$ GeV. Events with zero jets ($p_{\text{T}}^{jet} > 25$ GeV) are only considered. Figure 4(a) shows transverse energy distribution for photon. The measured cross section has significance 1.4σ and is an agreement with NLO predictions by VBFNLO within statistical uncertainty.

Semi-leptonic $WV\gamma$ events with one leptonically decaying W boson and one hadronically decaying W or Z boson are studied. Signal events are required to have $E_{\text{T}}^{\text{miss}} > 30$ GeV, one isolated photon with $E_{\text{T}}^{\gamma} > 15$ GeV, one electron or one muon with $p_{\text{T}} > 25$ GeV and $m_{\text{T}} > 30$ GeV. Events with at least two jets (not b-jets) and $70 < m_{jj} < 100$ GeV are considered. Figure 5 shows upper exclusion limits on production cross-section for all studied channels. The observed limits are between 1.8 and 4.1 times larger than the SM cross-section.

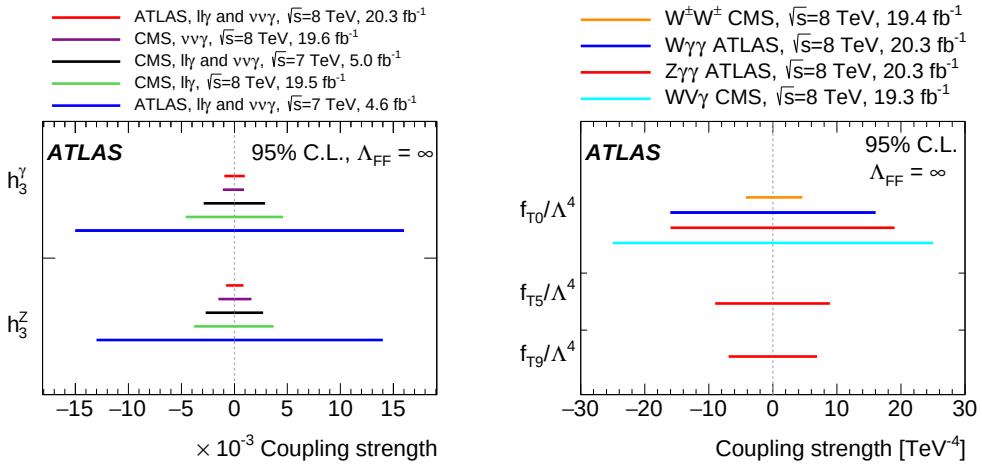

(a) (b)

Fig. 6: Comparison of the observed from $Z\gamma$ analysis ununitarized limits for the aTGC parameters (h_3^γ and h_3^Z) with previous ATLAS and CMS results (left), and comparison of the observed from $Z\gamma\gamma$ analysis ununitarized limits for the aQGC parameters (f_{T0}/Λ^4, f_{T5}/Λ^4 and f_{T9}/Λ^4) with previous ATLAS and CMS results (right) [5].

	Limits 95% CL	Measured [TeV^{-4}]	Expected [TeV^{-4}]
ATLAS $Z(\to \ell\bar{\ell}/\nu\bar{\nu})\gamma$-EWK	f_{T9}/Λ^4	$[-3.9, 3.9]$	$[-2.7, 2.8]$
	f_{T8}/Λ^4	$[-1.8, 1.8]$	$[-1.3, 1.3]$
	f_{T0}/Λ^4	$[-3.4, 2.9]$	$[-3.0, 2.3]$
	f_{M0}/Λ^4	$[-76, 69]$	$[-66, 58]$
	f_{M1}/Λ^4	$[-147, 150]$	$[-123, 126]$
	f_{M2}/Λ^4	$[-27, 27]$	$[-23, 23]$
	f_{M3}/Λ^4	$[-52, 52]$	$[-43, 43]$
CMS $Z(\to \ell\bar{\ell})\gamma$-EWK	f_{T9}/Λ^4	$[-4.0, 4.0]$	$[-6.0, 6.0]$
	f_{T8}/Λ^4	$[-1.8, 1.8]$	$[-2.7, 2.7]$
	f_{T0}/Λ^4	$[-3.8, 3.4]$	$[-5.1, 5.1]$
	f_{M0}/Λ^4	$[-71, 75]$	$[-109, 111]$
	f_{M1}/Λ^4	$[-190, 182]$	$[-281, 280]$
	f_{M2}/Λ^4	$[-32, 31]$	$[-47, 47]$
	f_{M3}/Λ^4	$[-58, 59]$	$[-87, 87]$
CMS $W(\to \ell\nu)\gamma$-EWK	f_{T0}/Λ^4	$[-5.4, 5.6]$	$[-3.2, 3.4]$
	f_{M0}/Λ^4	$[-77, 74]$	$[-47, 44]$
	f_{M1}/Λ^4	$[-125, 129]$	$[-72, 79]$
	f_{M2}/Λ^4	$[-26, 26]$	$[-16, 15]$
	f_{M3}/Λ^4	$[-43, 44]$	$[-25, 27]$

Fig. 7: Comparison of the observed ununitarized limits for the aQGC parameters in the Zγ VBS analysis with CMS results [6].

2.4 Anomalous triple and quartic gauge couplings

Vector-boson self-interactions are completely fixed by the model's $SU(2)_L \times U(1)_Y$ gauge structure. Their observation is thus a crucial test of the model. Anomalous coupling parameters can parameterize possible deviations from the SM at high E_{T} [8, 9].

Anomalous TGC in $Z\gamma$ channels, which vanish in the SM at tree level, are studied using vertex approach. The dominant contribution from aTGC is expected for region with high-E_{T} photons therefore the study is done in region with $E_T^\gamma > 250$ GeV for charged channels and with $E_{\mathrm{T}}^\gamma > 400$ GeV for neutrino channel. Having found no significant deviations from SM predictions, the data are used to set limits on anomalous triple couplings of photons to Z bosons. Figure 6(a) shows the experimental ununitarized limits for studied aTGC parameters and comparison with CMS and previous ATLAS results.

Other analyses described in Section 2.1 used data to search for aQGC. An effective field theory with higher-dimensional operators is adopted to parameterize these anomalous couplings. Figure 4(b)

summarizes expected and observed ununitarized limits for all studied parameters in $WV\gamma$ study. In this analysis first exclusion limits on the coupling parameters $f_{\text{M4,M5}}$ and $f_{\text{T6,T7}}$ are obtained. Neutral quartic couplings are not present in SM. Signal yields from $Z\gamma\gamma$ channels is used to set limits on parameters $f_{\text{M2,M3}}$ and $f_{\text{T0,T5,T9}}$. To maximize aQGC sensitivity in $Z\gamma\gamma$ channel similarly to $Z\gamma$ a region with high invariant mass of two photons ($m_{\gamma\gamma}$) is considered: $m_{\gamma\gamma}$> 200 GeV for charged channel and $m_{\gamma\gamma}$> 300 GeV for neutrino channel. Figure 6(b) shows corresponding ununitarized limits together with results obtained by other experiments. Limits from VBS analysis are shown on figure 7 and compared to CMS results. The neutrino channel provides best expected limits for all studied operators. Combination with charged channels improves results by 5-10%. ATLAS and CMS limits for aQGC parameters obtained using $Z\gamma$ scattering process are of the same order.

3 Conclusion

ATLAS provides great opportunities to study $V\gamma(\gamma)$ productions in high energy proton-proton collisions with previously unattainable accuracy. All measurements reported here demonstrate an agreement with the theory predictions. No evidence for physics beyond the SM is found in anomalous boson triple and quartic couplings at the level of statistics obtained at LHC during the first data-taking period.

Acknowledgments

This work was performed within the framework of Nuclear Physics and Engineering Institute and supported by MEPhI Academic Excellence Project (contract 02.a03.21.0005 of 27.08.2013)

References

[1] ATLAS Collaboration, *The ATLAS Experiment at the CERN Large Hadron Collider*, *JINST* **3** (2008) S08003.

[2] Evans, Lyndon and Bryant, Philip, *LHC Machine*, *JINST* **3** (2008) S08001.

[3] J. M. Campbell, R. K. Ellis and C. Williams, *Vector boson pair production at the LHC, JHEP* **07** (2011) 018, arXiv:1105.0020[hep-ph].

[4] M. Grazzini, S. Kallweit and D. Rathlev, *$W\gamma$ and $Z\gamma$ production at the LHC in NNLO QCD, JHEP* **07** (2015) 085, arXiv:1504.01330[hep-ph].

[5] ATLAS Collaboration, *Measurements of $Z\gamma$ and $Z\gamma\gamma$ production in pp collisions at $\sqrt{s} = 8$ TeV with the ATLAS detector*, *Phys. Rev.* **D 93** (2016) 112002, arXiv:1604.05232[hep-ph], http://atlas.web.cern.ch/Atlas/GROUPS/PHYSICS/PAPERS/STDM-2014-01/.

[6] ATLAS Collaboration, *Studies of $Z\gamma$ electroweak production in association with a high-mass di-jet system in pp collisions at $\sqrt{s}$ = 8 TeV with the ATLAS detector*, *JHEP* **07** (2017) 107, arXiv:1705.01966[hep-ex].

[7] ATLAS Collaboration, *Study of $WW\gamma$ and $WZ\gamma$ production in pp collisions at $\sqrt{s}$=8 TeV and search for anomalous quartic gauge couplings with the ATLAS experiment*, arXiv:1707.05597[hep-ex]

[8] U. Baur and Edmond L. Berger, *Probing the weak boson sector in $Z\gamma$ production at hadron colliders, Phys. Rev.* **D 47** (1993) 4889.

[9] C. Degrande, N. Greiner, W. Kilian, O. Mattelaer, H. Mebane, T. Stelzer, S. Willenbrock and C. Zhang, *Effective Field Theory: A Modern Approach to Anomalous Couplings, Annals Phys.* **D 335** (2013) 21, arXiv:1205.4231[hep-ph].